JOURNAL OF APPLIED ELECTROCHEMISTRY 17 (1987) 789–799

Low-temperature charging behaviour of lead–acid cells

T. F. SHARPE, R. S. CONELL

Electrochemistry Department, General Motors Research Laboratories, Warren, Michigan 48090, USA

Received 17 September 1986; revised 15 November 1986

The effect of temperature on the charging behaviour of lead–acid cells was studied at a depth of discharge of ~20% of their reserve capacity. As expected the charge acceptance rates dropped markedly at temperatures below 0° C. The ability to charge at these temperatures was limited by a precipitous increase in polarization at the negative plates which occurred immediately upon starting the charge. At −18° C the charge acceptance rates fell within a range of 20 to 40% of that observed at 25° C. The highest rates at −18° C were favoured where the charge followed a high-rate, low-temperature discharge, with a minimum time and temperature for the open circuit stand. We speculate that this is due to factors such as a small $PbSO_4$ crystal size and a non-equilibrium electrolyte concentration in the pores of the plates. Direct evidence for this is lacking, however, because of the need for *in situ* determination of the physical structure of the plates in the discharged condition.

1. Introduction

In automotive application, the alternator charges the lead–acid battery at a set voltage with an upper current limit [1]. As full state of charge is reached, the counter e.m.f. of the battery rises to the voltage setting, thereby diminishing the charging current. However, at ambient winter temperatures (≦0° C) the counter e.m.f. rises at a faster rate than at warmer temperatures, so that the charging current may diminish before full state of charge is reached.

In electrochemical terms, the battery has a greater tendency to become polarized during charging current flow as the temperature is decreased. The polarization behaviour is governed by the individual polarization characteristics of the positive and negative plates within the battery cell elements. (In this paper, polarization refers to the measured departure from open circuit voltage during the charge.) The use of a higher voltage setting to force current beyond the polarization limit could cause adverse side effects, such as gassing at the plates.

The present work is concerned with the monitoring of charge input at temperatures between the extremes of 25° C and −18° C, in order to observe the changing pattern in positive and negative plate polarization as a function of charging temperature. Charge input was also monitored at a fixed low temperature (−18° C), following variations in the discharge rate (current) and temperature, as well as open circuit stand time and temperature between discharge and charge. These variations provide different mass transport conditions for the charge and therefore provide further insight to the reasons for lower charge acceptance rates as the temperature decreases.

2. Experimental details

All testing was carried out on single cell elements of a nominal reserve capacity of 75 min, whose plates (five positives, four negatives) were 11.0 × 13.7 cm. For all the tests the cells in the fully charged condition were discharged for 405 A min (to a depth of ~20% of the reserve capacity), either at a low rate (25 A for 16.2 min) or a high rate (two 30-s, 405-A discharges with an intervening 2 min rest). Charging was performed at a setting of 2.64 V, with a maximum current setting of 25 A. The 'external sensing' feature of the Hewlett–Packard 6268B power

0021–891X/87 $03.00 + .12

supply was used to eliminate the effect of ohmic losses in the charging circuit.

The positive and negative plate polarizations during charge were obtained against a Hg/Hg_2SO_4 reference electrode. The reference electrode capillary was positioned between the innermost positive plate and the separator bag containing the adjacent negative plate. Its tip was located at the plate centre, although a few measurements were made on a cell with multiple reference electrodes, where the capillary tips were positioned either within the upper third, at the centre, or within the lower third section of the plates. It was found, however, that the polarization measurements on charge did not vary significantly as a function of capillary tip location. As expected, the sum of the positive and negative plate polarizations equalled the measured cell polarization.

Cell current and all voltages were monitored by a Fluke 2240B data logger, where readings were obtained every 3–5 s for the first 3 min of charge and about every 2 min thereafter. The gas evolution rate on charge was monitored through 3.2 mm i.d. polypropylene tube extending through the cell top, using a standard Matheson mass flowmeter.

Temperature was measured by a Cr–Al thermocouple placed between the innermost plates of the cells. The temperatures stated in this work are those registered at the start of a charge or discharge. It is to be noted that, from a starting temperature of $-18°$ C, the temperature rise during a discharge at 25 A or during a charge was only about 2° C. However, from an initial temperature of $-18°$ C the temperature rise was as much as 15° C during discharge at 405 A. The time required for a cell to re-equilibrate to $-18°$ C following such a discharge was 50 min.

3. Results

3.1. *Effect of temperature on charge*

We first varied the charging temperature, keeping the previous discharge conditions and the open-circuit stand time constant. The procedure for each test was

(i) Overnight ($\sim$ 16 h) open circuit stand in fully charged condition at $-18°$ C.

(ii) Discharge at 405 A (two 30-s discharge intervals with an intervening rest of 2 min).

(iii) Overnight ($\sim$ 16 h) open-circuit stand at the indicated charging temperature.

(iv) Charge at 2.64 V/25 A maximum current.

The current input, charge input, cell polarization and gassing rates at the various charging temperatures are shown in Figs 1–4, respectively.

The broken line in Fig. 2 represents full charge input, based on the capacity that was drawn from the cell in the previous discharge (405 A min). For the charge at 25° C the input exceeds this value because of the side reaction of gassing* (Fig. 4). With a decrease in charging temperature the cell polarization increases (Fig. 3), so that the charging current is diminished (Fig. 1). Positive and negative plate components of the cell polarization are shown later.

3.2. *Effect of previous discharge rate (current) and temperature on charge at $-18°$ C*

Results comparing the charge input at $-18°$ C (from Fig. 2) to the charge input at that temperature, when we varied the temperature and rate of the previous discharge, are shown in Fig. 5. Here it is seen that the higher charge input rates are obtained following decreasing discharge temperature and increasing discharge rate.

3.3. *Effect of open-circuit stand time and temperature on charge at $-18°$ C*

Fig. 6 shows the influence of open-circuit stand time between a low-temperature discharge and charge. The shortest time shown was the time required for the cell to re-equilibrate to $-18°$ C following the discharge. A decrease in charge acceptance rate is observed with increasing open-circuit stand time.

Fig. 7 shows that a yet further decrease in charge acceptance rate is obtained if the temperature of the cell is simply allowed to increase between the discharge and charge. Curve a,

* Under field conditions, this gassing would not occur because the alternator setting is temperature compensated. However, to avoid an additional variable in the testing, a setting of 2.64 V was used for all charging temperatures. This corresponds to a typical setting for the alternator at $-18°$ C.

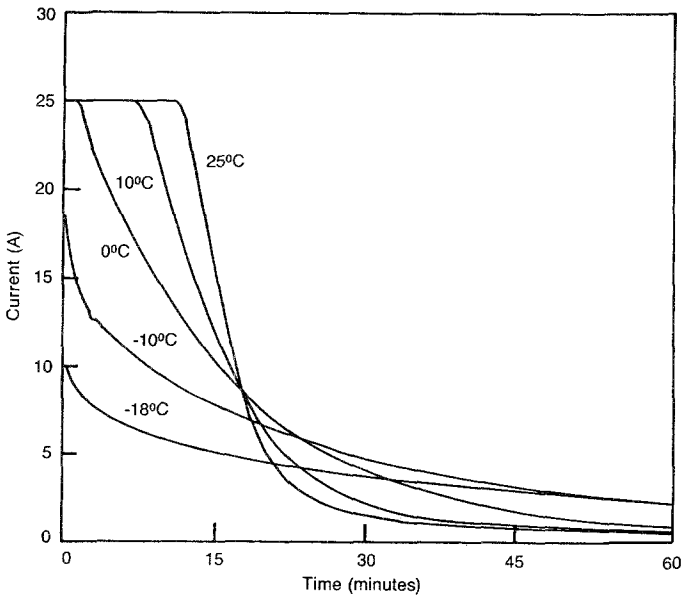

Fig. 1. Current input for a 2.64 V/25 A charge at various temperatures. Charge was preceded by 405 A discharge at −18° C, plus an overnight stand at the indicated charging temperature.

which was obtained after an overnight open circuit stand at −18° C is to be compared to a lower charge input rate (curve b), when the temperature of the cell had been allowed (following the discharge) to increase to room temperature (~25° C) before the overnight open circuit stand at −18° C. Curve c, which was obtained after a one-week open circuit stand at −18° C, is to be compared to a lower charge input rate (curve d), when the temperature of the cell was allowed (following the discharge) to increase to room temperature and then stand for 6 days before an overnight stand at −18° C.

3.4. *Plate polarization measurements*

The positive and negative plate components of the cell polarization (Fig. 4) as a function of charging temperature are shown in Fig. 8 (for 25° C and 10° C) and in Fig. 9 (for 0° C, −10° C

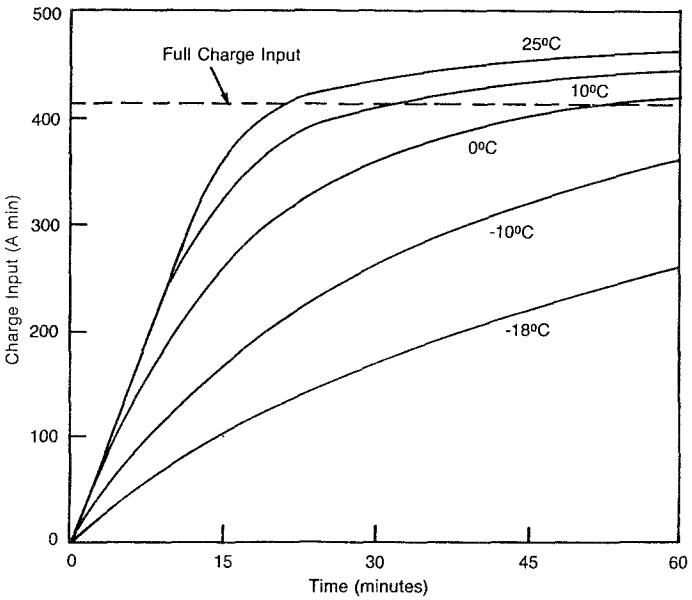

Fig. 2. Charge input for conditions stated in Fig. 1.

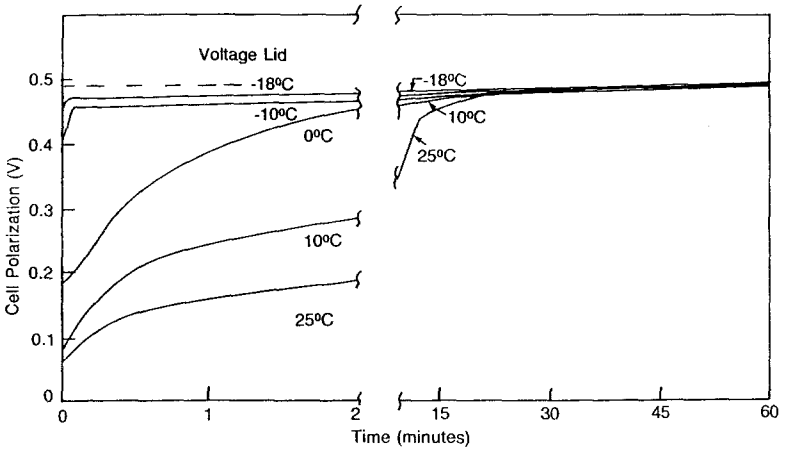

Fig. 3. Cell polarization for conditions stated in Fig. 1.

and −18° C). The plate polarization curves for a 25° C charge are similar to those reported in the literature [2]. Here, the positive plates account for most of the cell polarization up to the point where the polarization at the negative plates increases, which indicates that they are becoming fully charged. With the tapering of the charging current the positive plate polarization decays, but this happens at a slow rate, presumably because of the slowness of obtaining an equilibrium concentration of electrolyte within the porous plate structure. The profile observed at 10° C is similar, although there is an increase in both positive and negative plate polarization. With the further lowering of charge temperature, Fig. 9 shows that the abrupt jump in polarization, which diminishes the charge, occurs at the negative plates.

The positive and negative plate polarization traces for the spectrum of charge inputs shown in Figs 5–7 were all qualitatively similar to the profile shown for the −18° C charge in Fig. 9c. Differences, however, in the specific values of the distribution of polarization between the positive and negative plates could be correlated to variations in the charge input. Plate polarization profiles for the highest charge input and the lowest charge input are shown in Fig. 10. Plate polarizations for the intermediate charge inputs fell between these extremes. To demonstrate this

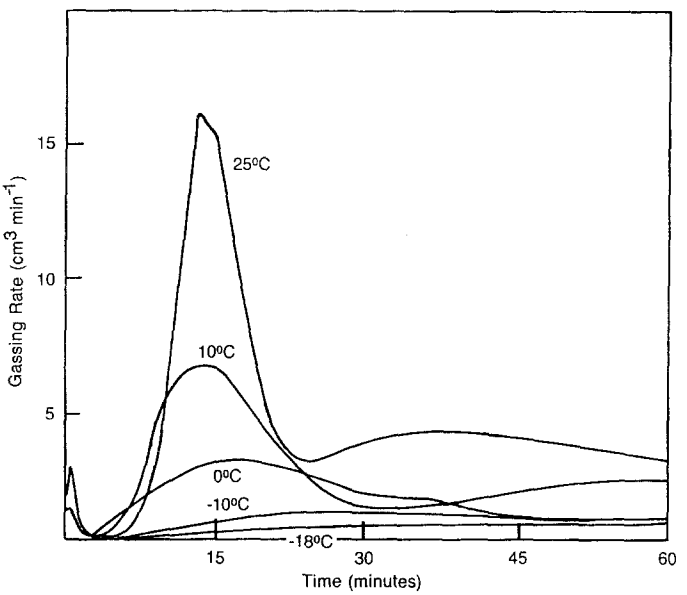

Fig. 4. Gassing rates for conditions stated in Fig. 1.

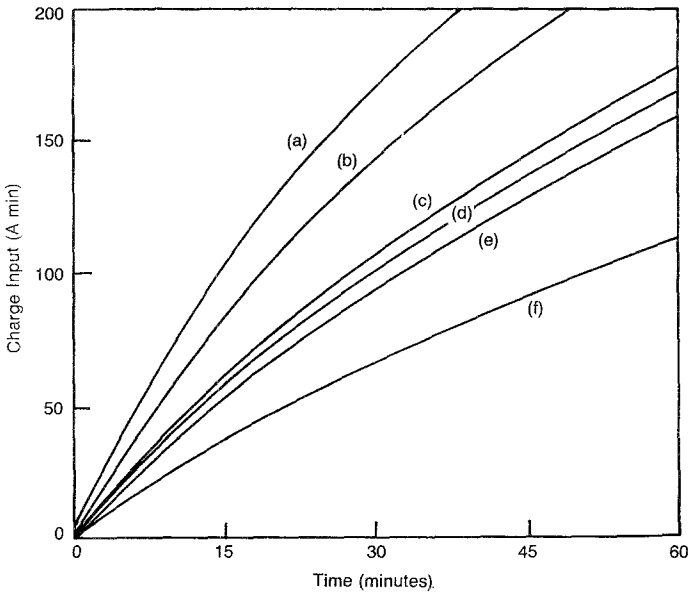

Fig. 5. Charge input at −18° C, where temperature and rate of previous discharge are variables. Between discharge and charge, the cell stood overnight on open circuit at −18° C. Previous discharge: (a) 405 A, −18° C, 1.0 min; (b) 405 A, 0° C, 1.0 min; (c) 405 A, 25° C, 1.0 min; (d) 25 A, −18° C, 16.2 min; (e) 25 A, 0° C, 16.2 min; (f) 25 A, 25° C, 16.2 min.

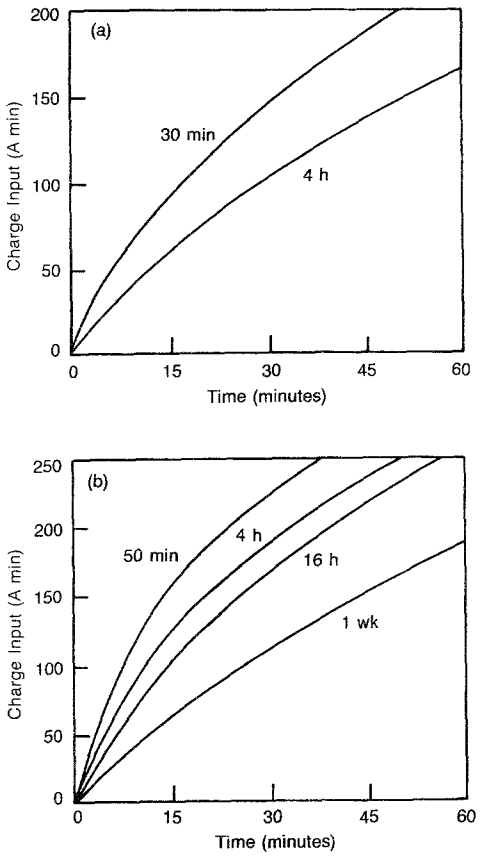

Fig. 6. Charge input following (a) 25 A and (b) 405 A discharges at −18° C, where open-circuit stand time between discharge and charge is a variable.

trend, Fig. 11 shows the charge input versus a resistance value, obtained by dividing the plate polarization by the current at 40 s into the charge. Here it is seen that the variation of charge input rate with previous discharge and open-circuit stand conditions is related to a change in resistance of over an order of magnitude at the negative plates, but to a much smaller change at the positive plates.

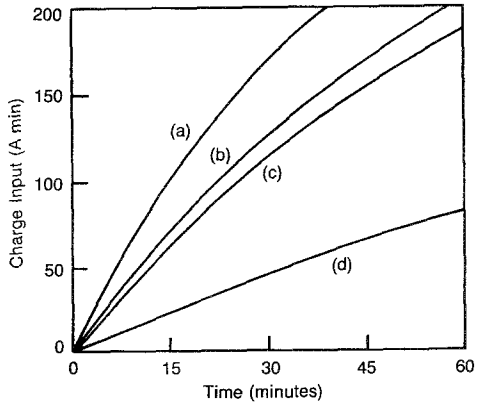

Fig. 7. Charge input at −18° C, following: (a) 405 A discharge at −18° C, plus overnight open circuit stand at −18° C; (b) 405 A discharge at −18° C, then an increase in cell temperature to 25° C over a ~5 h interval before overnight open circuit stand at −18° C; (c) 405 A discharge at −18° C, plus open circuit stand for one week at −18° C; (d) 405 A discharge at −18° C, plus open circuit stand for 6 days at 25° C plus overnight open circuit stand at −18° C.

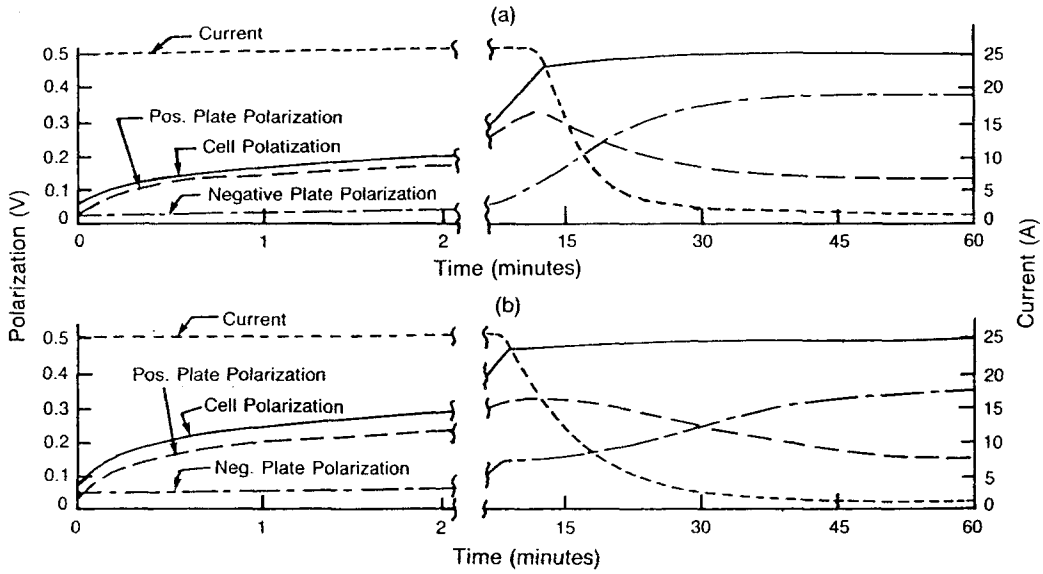

Fig. 8. Current and polarization profiles for charges at (a) 25° C and (b) 10° C, under conditions specified in Fig. 1.

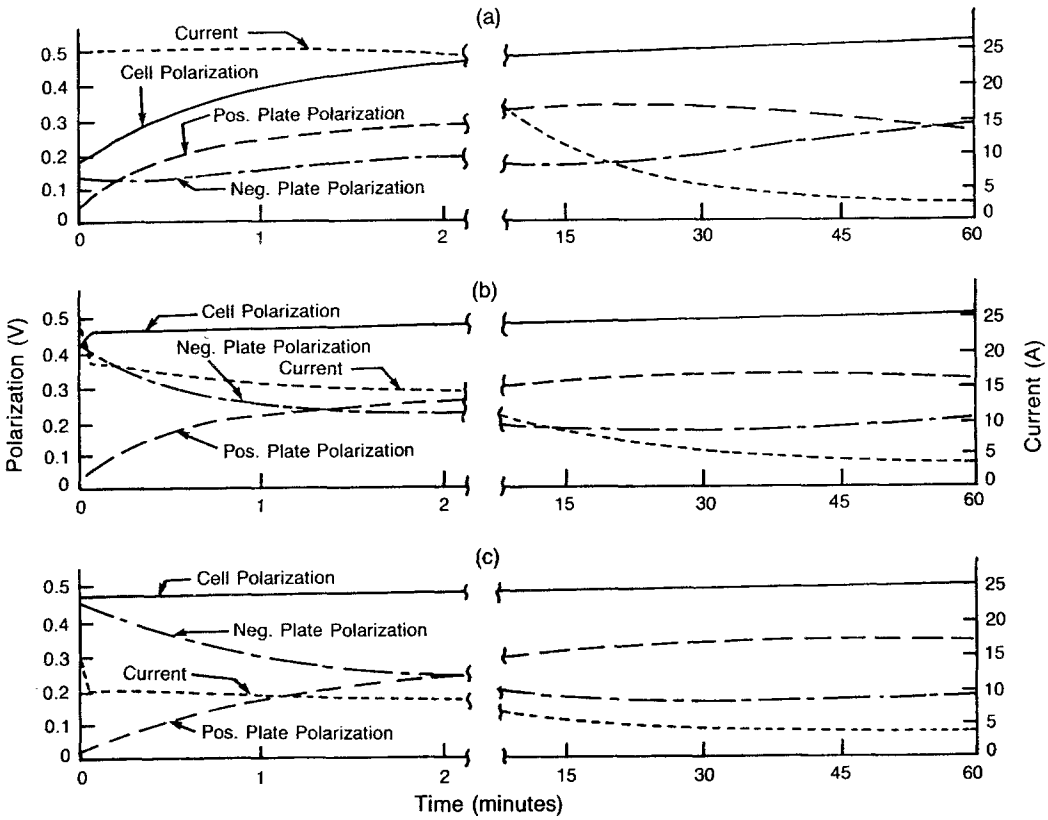

Fig. 9. Current and polarization profiles for charges at (a) 0° C, (b) −10° C, and (c) −18° C, under conditions specified in Fig. 1.

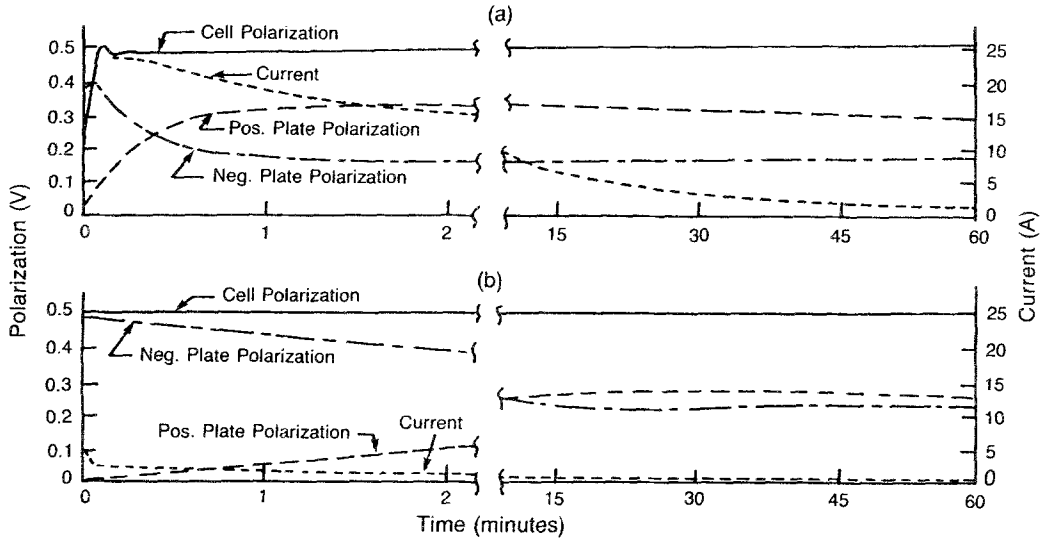

Fig. 10. Charging profiles for (a) highest charge input (Fig. 6) and (b) lowest charge input (Fig. 7) that was obtained at −18° C.

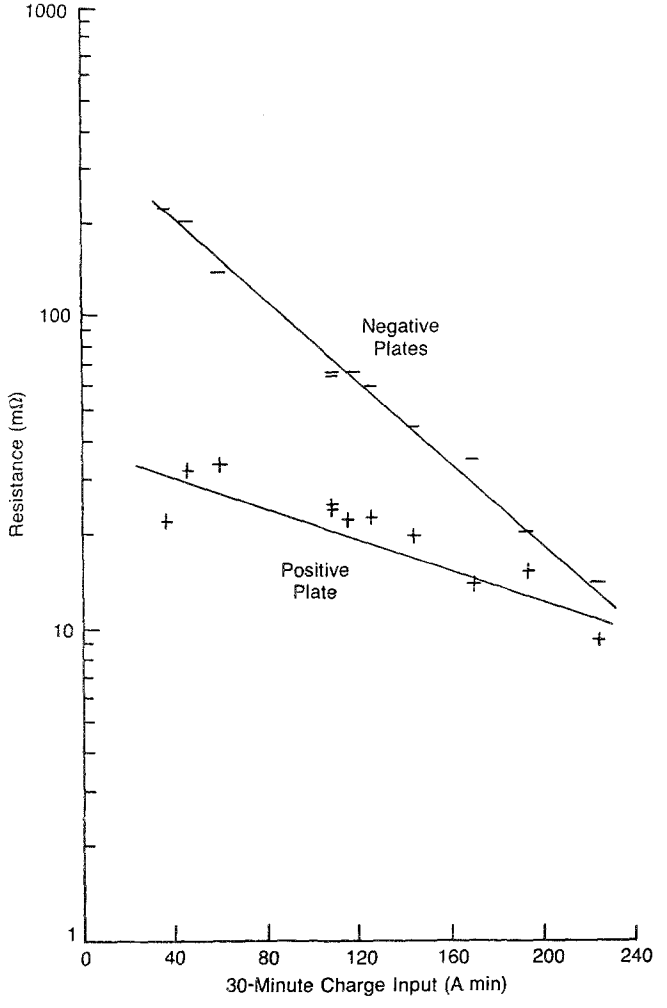

Fig. 11. Positive plate and negative plate resistance values obtained at 40 s into each of the charges shown in Figs 5–7.

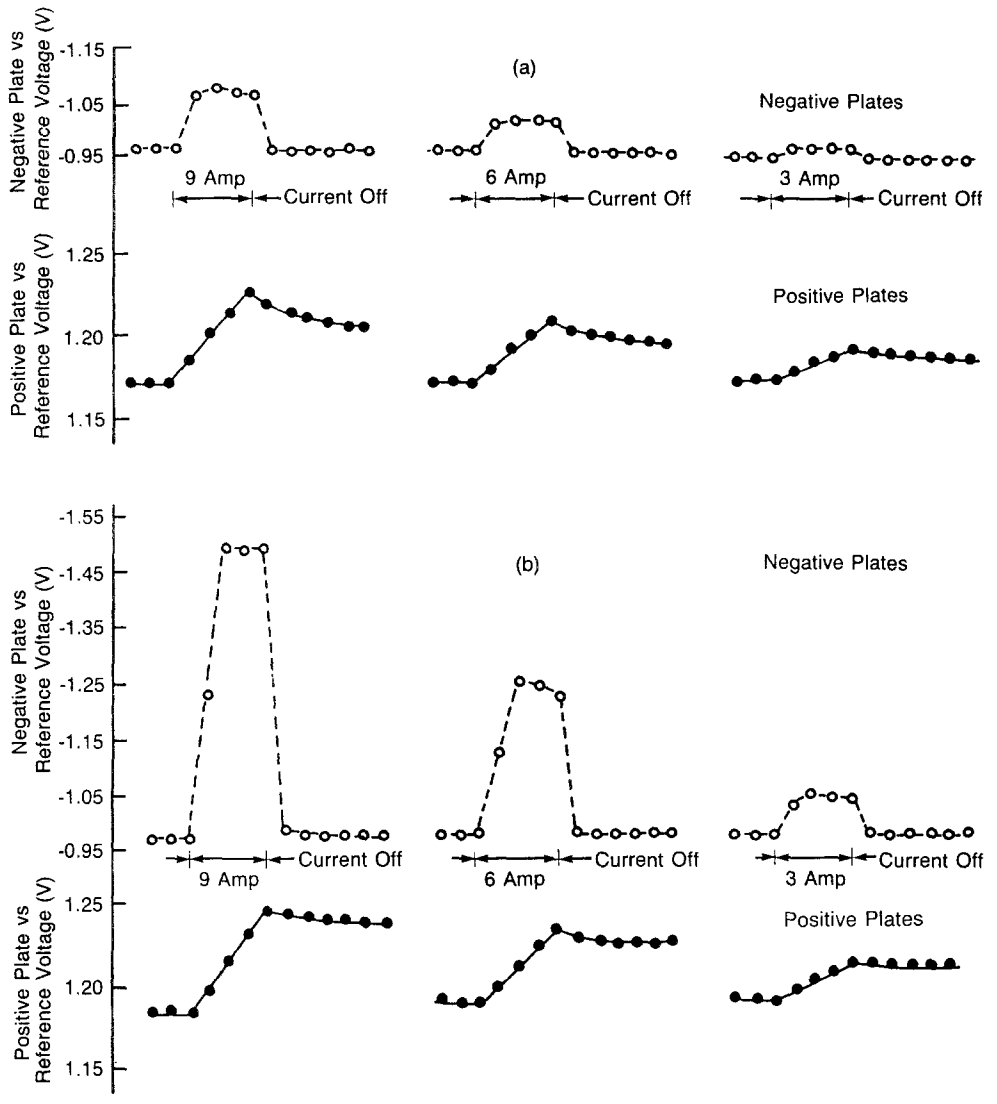

Fig. 12. Plate responses to charging current pulses (15 s) at −10°C, following (a) 25 A discharge at 25° C, plus overnight stand at −10° C, or (b) 405 A discharge at −18° C, plus overnight stand at −10° C. (Time between pulses was 30 min).

3.5. *Constant current charging*

A complication during charging at a set voltage is that current varies with charging time. To obtain a more straightforward dependence of plate polarization on current, the build-up and decay of plate polarization was measured with the application of constant current charging pulses. These pulses were applied at the 20% depth of discharge, following either of two discharge conditions; namely (i) 25 A at 25° C, followed by overnight stand at the charging temperature, or (ii) 405 A at −18° C, followed by overnight stand at the charging temperature. The pulses were applied at 0, −5, −10 and −18° C, but for brevity, only pulses at −10° C are shown in Fig. 12. At each temperature it was observed that all of the negative plate polarization builds and decays within the first few seconds of switching on or off the current, whereas that for the positive plate builds and decays more slowly.

The relationship between applied current and the magnitude of plate polarization (the difference between open circuit voltage and voltage at end of pulse) at the end of the current pulses is

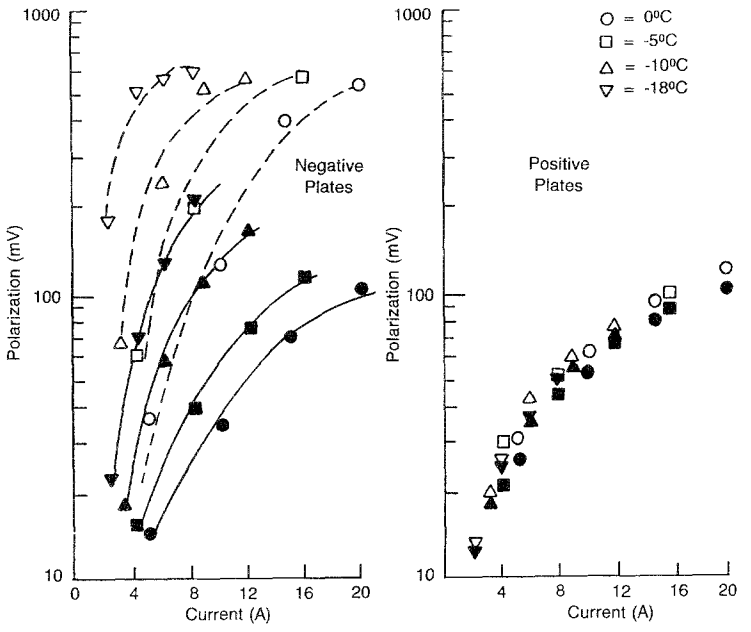

Fig. 13. Plate polarizations at the end of the constant current charging pulses typified by Fig. 12. The open data symbols correspond to previous discharge conditions specified for Fig. 12a, whereas the solid data symbols correspond to previous discharge conditions specified for Fig. 12b.

shown in Fig. 13. These results (a) reaffirm that the negative plate polarization is highly sensitive to both charging temperature and the conditions of previous discharge, and (b) show that no gain in charge acceptance rate would be expected through positive plate modification, because a potentially higher charge current would lead to an exponential increase in negative plate polarization at the onset of charge.

4. Discussion

This work has shown a spectrum of charge input rates at low temperature depending on the conditions (rate and temperature) of the previous discharge.

During the discharge the electrolyte in the pores of the plates becomes diluted as sparingly soluble $PbSO_4$ is precipitated in the pores and on the surface of the plates. For the recharge the $PbSO_4$ must first dissolve, therefore higher charge rates would be expected under conditions where the $PbSO_4$ crystal size is the smallest. This could explain why the highest charge rates at $-18°C$ were obtained following a high-rate, low-temperature discharge, since $PbSO_4$ crystal size at negative plates has been reported [3, 4] to decrease in proportion to increasing discharge current and decreasing discharge temperature. The highest charge rates also followed the shortest times and lowest temperatures for the open-circuit stand between discharge and charge. This could be because with a short open-circuit stand at minimum temperature, the $PbSO_4$ does not have an opportunity to recrystallize to bring about a decrease in its surface area. Another consideration is that a higher solubility of $PbSO_4$ in the pores of the plates would be favoured immediately following a discharge, i.e. before the electrolyte in the pores has had time to equilibrate with the bulk electrolyte.

To confirm these hypotheses, a direct determination of the physical structure of the plates prior to charging would be needed. This, however, would require the development of *in situ* techniques. Any *ex situ* investigation would not be expected to provide a one-to-one correlation to the condition of the plates in the cell environment, particularly if the $PbSO_4$ is undergoing recrystallization. With the customary SEM investigation, speculation also arises because of the need to wash the plates. It has been shown [5] that the washing procedure changes the distribution of $PbSO_4$ in the plates, and it is presumed that the washing dissolves some of the $PbSO_4$.

The charge input rates at low temperature, although showing marked variation depending on the previous discharge and open-circuit stand conditions, were consistently limited by a

precipitous increase in negative plate polarization at the onset of charge. This could be due to the $PbSO_4$ dissolution rate not keeping up with the reduction of Pb^{2+} to Pb, or to a slowness in the diffusion rate of Pb^{2+} to reduction sites. More sophisticated techniques with well-characterized lead electrodes would be required to distinguish between these or other possibilities as rate-controlling steps. Expander formulations, although necessary to provide cold temperature cranking ability, may have the adverse side effect of inhibiting the charge at low temperatures. Recent rotating ring-disc studies [6] on smooth lead electrodes suggest that Pb^{2+} deposition sites can be blocked by the presence of expander.

During the initial moments when the charging current is passing through the plate interfaces, the electrochemical oxidation and reduction reactions are shunted out because of the build-up of double-layer capacitance. Extensive treatment of double-layer charging in battery plates can be found elsewhere [7, 8].

The constant current transients in Fig. 12 suggest that during the complete build-up of negative plate polarization the positive plates are within the time-frame for double-layer charging. This is indicated by the linear increase in positive plate polarization during the 15-s pulses. The double-layer capacity, C_{dl}, in farads, calculated from

$$C_{dl} = i\left(\frac{dt}{dv}\right)$$

where i = applied current (A), t = time (s) and v = polarization (V), is given in Table 1. The values obtained are somewhat lower than literature values for positive plates (normalized with respect to our positive plate dimensions), namely $2.7\,F\,cm^{-2}$ [7] and $5.8\,F\,cm^{-2}$ [8]. The latter authors, however, evacuated their cells to remove entrapped gases prior to the capacity measurements, a procedure that we did not use. They pointed out that entrapped gases may lead to low values for the double-layer capacity.

Double-layer charging for the negative plates was not resolved in this work. It would fall well within the minimum response time of the data logger, since double-layer capacities for negative plates are at least an order of magnitude smaller than those for the positive plates [7, 8].

Table 1. Double-layer capacities for positive plates calculated from constant current charging transients (a) following a 25 A, 25° C discharge, and (b) following a 405 A, −18° C discharge

Temperature (° C)	i *(A)*	t *(s)*	dv *(V)*		C *(F cm^{-2})*[a]	
			(a)	*(b)*	*(a)*	*(b)*
−18	8	15	0.050	0.053	2.0	1.9
	6	15	0.037	0.040	2.0	1.9
	4	15	0.025	0.026	2.0	1.9
	2	15	0.015	0.013	1.7	1.9
−10	12	15	0.077	0.075	1.9	2.0
	9	15	0.062	0.056	1.8	2.0
	6	15	0.042	0.038	1.8	2.0
	3	15	0.020	0.017	1.9	2.2
−5	16	15	0.101	0.095	2.0	2.1
	12	15	0.093	0.070	1.6	2.1
	8	15	0.052	0.044	1.9	2.3
	4	15	0.025	0.020	2.0	2.5
0	20	15	0.124	0.107	2.0	2.3
	15	15	0.097	0.082	1.9	2.3
	10	15	0.065	0.054	1.9	2.3
	5	15	0.030	0.025	2.1	2.5

[a] Positive plate area in cell = $1206\,cm^2$.

Acknowledgement

The authors are indebted to N. Eisenhut and S. Dasgupta of Delco-Remy Division, Anderson, Indiana, for supplying the cell elements for this study.

References

[1] H. Bode, 'Lead Acid Batteries', Wiley, New York (1977) Fig. 4.14(c), p. 308.

[2] W. G. Sunu and B. W. Burrows, 'Electrolyte Stratification and Charge Characteristics of Industrial Lead–Acid Cells', Power Sources 6, Academic Press, London and New York (1975) p. 601.

[3] C. P. Wales, S. M. Caulder and A. C. Simon, *J. Electrochem. Soc.* **128** (1981) 236.

[4] E. M. L. Valeriote, Defense Research Establishment Ottawa Technical Note No. 79–24, reproduced by National Technical Information Service, US Dept of Commerce, Springfield, VA 22161 (October, 1979).

[5] D. Simonsson, *J. Electrochem. Soc.* **120** (1973) 151.

[6] G. Hoffmann and W. Vielstich, *J. Electroanal. Chem.* **180** (1984) 565.

[7] P. Ruetschi, J. B. Ockerman and R. Amlie, *J. Electrochem. Soc.* **107** (1960) 325.

[8] W. Tiedemann and J. Newman, *ibid.* **122** (1975) 70.